Detecting palladium nanoparticles in Pd/C catalysts using X-ray Rietveld method

G. Fagherazzi [a], P. Canton [a], P. Riello [a], F. Pinna [b] and N. Pernicone [c]

[a] *Dipartimento di Chimica Fisica, Università di Venezia, DD2137, 30123 Venezia, Italy*
E-mail: fagheraz@unive.it
[b] *Dipartimento di Chimica, Università di Venezia, DD2137, 30123 Venezia, Italy*
[c] *Consultant, Via Pansa 7/c, 28100 Novara, Italy*

Received 9 August 1999; accepted 15 December 1999

This study uses X-ray diffraction (XRD) techniques to investigate the nanostructural features of a series of four Pd/C catalysts, which had the same load, 0.51 ± 0.02 wt%, as palladium, with significantly different dispersions, obtained by applying different temperature ageings up to 873 K. By means of a Rietveld refinement, performed using a special fitting procedure, which takes into account the various contributions to the background scattering, the palladium fraction due to nanoparticles or clusters smaller than about 20–25 Å could be determined. We have compared this Rietveld (absolute) quantitative method with a simpler, but less precise, single-peak (relative) XRD analysis, interesting for fast industrial applications. The Pd fractions due to nanoparticles, as determined by the two methods, are close each other for all samples investigated, apart from one for which the disagreement is near 20%.

Keywords: Pd/C catalysts, nanostructural features, nanoparticles, nanoclusters, X-ray diffraction, Rietveld analysis

1. Introduction

Detecting and measuring the nanoparticle size of active phases in metal supported catalysts is very important for a full characterization of the complex nanostructure of these composite materials, which is strictly connected to their catalytic behaviour [1,2].

When utilizing XRD (X-ray diffraction) some of us have recently observed [3] in Pd/C catalysts that, although the metal concentration was nearly the same (∼0.5 wt%) and the experimental conditions constant, the Pd peak intensities changed very significantly, sample by sample. As a matter of fact, strong decreases in the Pd(111) peak intensities were observed in a series of Pd/C catalysts, when metal dispersion increased. As crystal preferred orientation has to be excluded for small very dispersed spheroidal particles (as will be confirmed by the present Rietveld analysis itself), this behaviour can be explained by the fact that the intensity lost by the Pd(111) peak had spread out into the background scattering. Therefore, we had assumed that this diffuse X-ray scattering originated from very thin palladium nanoparticles or nanoclusters (less than 20–25 Å in size). A conventional X-ray peak profile analysis is unable to evidence these nanoclusters, since they do not contribute to the Voigtian measurable X-ray diffraction peaks.

This paper examines the use of the Rietveld method in order to detect these nanoparticles and determine their weight fraction. A suitably tailored Rietveld analysis has recently been proposed [4] by some of us to determine the amount of each different phase present in a multi-phase semi-crystalline system, the amorphous phase amount included. This method is based on a previously proposed theoretical approach [5], which extended the classical Rietveld analysis [6]. Some examples of application on a few Au and Pd catalysts supported on active carbons have been recently published [7,8].

In this paper a much more systematic study is reported on a series of 0.5 wt% Pd/C catalysts having significantly different metal dispersions and crystallite sizes. It is worth noting that this type of catalysts is of industrial interest since they can be employed for the production of purified terephthalic acid. The results are compared with those obtained using the single-peak simplified method, which is particularly interesting for industrial applications.

2. Theory

After separating the intensity contributions $Y_l(2\theta)$ of each phase from the global scattering pattern of a multi-system of M phases, the fractional weight amount, W_l, of the lth phase, when the chemical compositions of these phases are known, becomes [4]

$$W_l = \frac{\mathsf{N}_l \sum_{i=1}^{n_l} w_l^i}{\sum_{l=1}^{M} \mathsf{N}_l \sum_{i=1}^{n_l} w_l^i} \tag{1}$$

with

$$\mathsf{CN}_l = \lim_{s_p \to \infty} CN_l(s_p) = \lim_{s_p \to \infty} \frac{\int_0^{s_p} (Y_l/AP)(s) s^2 \, \mathrm{d}s}{\sum_{i=1}^{n_l} \int_0^{\infty} \left[|f_i^0|^2 + I_i^{\mathrm{inc}} \right] s^2 \, \mathrm{d}s}, \tag{2}$$

where we have supposed that the composition unit of the lth phase is composed of n_l atoms and that the composition

units (e.g., the unit cells in the case of crystalline phases) in the lth phase are N_l; w_l^i is the atomic weight of the ith atom of the lth composition unit; A and P are the absorption and polarisation factors, respectively; f_i^0 is the tabulated atomic scattering factor; I_i^{inc} is the incoherent scattering of the ith atom: it can be evaluated using the analytical expression and the relevant parameters published by Smith et al. [9] and must be corrected for the Breit–Dirac factor, for specific absorption effects and for the band-pass function of the monochromator if it is used on the diffracted beam [10,11]; $s = 2\sin(\theta)/\lambda$, with 2θ Bragg angle and λ radiation wavelength; s_p is the upper experimental limit of measurement.

The proportionality constant, C, only depends on the measurement set-up when particle microabsorption effects can be ignored. For the nanometric particle sizes examined here, even if the difference between the mass absorption of palladium and that of carbon is very high, the conditions found by Brindley [12,13], in order to neglect microabsorption effects, are satisfied.

The value of W_l can be estimated by assessing the asymptotic mean value of the ratio $CN_l(s_p)$ in the range of $s_p > 1.0$ Å^{-1}.

In order to separate the palladium from the carbon scattering, the air corrected [14] diffraction pattern of the catalysts was fitted by using the palladium fcc structure and the experimental diffraction pattern of the active carbon employed as catalyst support (bi-phase model). We have used the following equation, based on our modified Rietveld approach [5]:

$$\begin{aligned} Y(2\theta) &= Y_{\text{Pd}}(2\theta) + Y_{\text{C}}(2\theta) \\ &= \left\{ K^{\text{Pd}} AP \left[\sum_{k=1}^{n_{\text{B}}} J_k L_k |F_k|^2 \Phi\left(2\theta^0 - 2\theta_k^0\right) + Y_{\text{Pd}}^{bk} \right] \right\} + K^{\text{C}} Y_{\text{C}}^*(2\theta), \end{aligned} \tag{3}$$

where

$$\begin{aligned} Y_{\text{Pd}}^{bk} = \frac{16\pi^2 V_{\text{c}}}{180\lambda^3} \Big\{ & 4 I_{\text{Pd}}^{\text{inc}} \\ & + 4\left[1 - \exp\left(-2B\sin^2(\theta)/\lambda^2\right)\right]\left[f_{\text{Pd}}^0\right]^2 \Big\} \end{aligned} \tag{4}$$

is the contribution to the background of the metal crystalline phase due to thermal and disorder scattering. The symbols are:

$Y(2\theta)$	air-corrected global intensity;
$Y_{\text{Pd}}(2\theta)$	air-corrected intensity contribution of Pd to the global intensity;
$Y_{\text{C}}^*(2\theta)$	air-corrected smoothed experimental carbon scattering from the pure support;
$Y_{\text{C}}(2\theta)$	air-corrected and suitably scaled carbon scattering;
K^{Pd}	palladium scale factor;
K^{C}	carbon scale factor;
n_b	number of reflections of palladium;
V_{c}	palladium unit cell volume, containing four atoms;
J_k	multiplicity factor;
L_k	Lorentz factor $1/\sin^2(\theta_k)\cos(\theta_k)$;
$\lvert F_k\rvert^2$	squared structure factor for the kth reflection, including the Debye–Waller factor;
$\Phi(2\theta^0 - 2\theta_k^0)$	normalised function (pseudo-Voigt, in the present analysis), describing the profile of the kth reflection, including asymmetry [15]; angles measured in degrees;
B	thermal factor for Pd atoms.

Since the integrated global intensities are independent of the atomic spatial ordering [16], equations (1) and (2) work *for both crystalline and amorphous phases*. In the case of crystalline phases, the integrated corrected intensity of the lth phase is related to the scale factor K^l, refined in the Rietveld procedure, as follows:

$$\begin{aligned} &\int_0^\infty I_l^{\text{corr}} 4\pi s^2 \,\mathrm{d}s \\ &\quad = K^l \frac{16\pi^2 V_{cl}}{180\lambda^3} \sum_{i=1}^{n_l} \int_0^\infty \left[\left|f_i^0\right|^2 + I_i^{\text{inc}}\right] 4\pi s^2 \,\mathrm{d}s, \end{aligned} \tag{5}$$

$$CN_l = \frac{16\pi^2}{180} \frac{1}{\lambda^3} K^l V_{cl},$$

where n_l is the number of atoms in the unit cell whose volume is V_{cl}. It is worth noting that equation (1) can be considered to be a generalization of the equation reported by Hill and Howard [6], found by them using a completely different theoretical approach, when all phases are crystalline.

The air-corrected carbon pattern used in the refinement was firstly fitted using a polynomial function of the fifth order and 6 pseudo-Voigt. This particular choice is not important: in fact we only wanted to smooth the function used in the Rietveld analysis.

3. Experimental

The "as received" catalyst (sample C_1) is a commercial catalyst (registered as D3065) by Chimet Co. (Arezzo, Italy). It is used for the industrial purification of terephthalic acid and is formed by a nominal 0.5 wt% of Pd, supported on active carbon. Effectively, the Pd concentration of this catalyst, as measured by the atomic absorption technique, has been found to be 0.51(2) wt%. Three other samples were prepared by thermally treating sample C_1 at the temperatures of 673 K (sample C_2), 773 K (sample C_3) and 873 K (sample C_4), for 24 h, in a controlled atmosphere of $H_2/H_2O = 1$.

XRD patterns were recorded at 295 K, with a step size of 0.05°, on a 10°–140° 2θ range. The intensities were collected in the preset-time mode in accordance with a specific program, which employed higher collection times in the angular ranges where the Pd peaks are defined, and lower times outside these ranges. The Rietveld program, which is an implemented version of the DBWS-9600 code written by

Sakthivel and Young [17], takes into account these different collection times when calculating the e.s.d. of the optimized parameters. A Philips X'Pert system (PW3020 vertical goniometer and PW3710 MPD control unit), equipped with a focusing graphite monochromator on the diffracted beam and with a proportional counter (PW1711/90) with an electronic pulse height discrimination, was used. Moreover, a divergence slit of 0.5°, a receiving slit of 0.2 mm, an anti-scatter slit of 0.5°, and Ni-filtered Cu Kα radiation (30 mA, 40 kV), were employed.

Air scattering Y^{air} was collected (10 s step^{-1} and step size of 0.5°) on the same 2θ range, fitted with a suitable function (two pseudo-Voigt functions and a straight line) and corrected in accordance with the method used by Ottani et al. [14] taking into account the presence of the sample. The scattering of the same active carbon powder used in the investigated Pd/C system, $Y_{\text{C}}^{*}(2\theta)$, was also corrected for air scattering before using it in the refinement. No change in the X-ray pattern of the carbon was observed, even when thermally treated up to 873 K.

4. Results and discussion

Figures 1 and 2 show the Rietveld refined diffraction patterns of the four investigated catalysts, whereas figure 3 shows the $CN_{\text{C}}(2\theta)$ plot as a function of 2θ, which refers to the active carbon scattering. Table 1 reports the palladium weight percentage, W_{Pd} (as calculated by equation (1)),

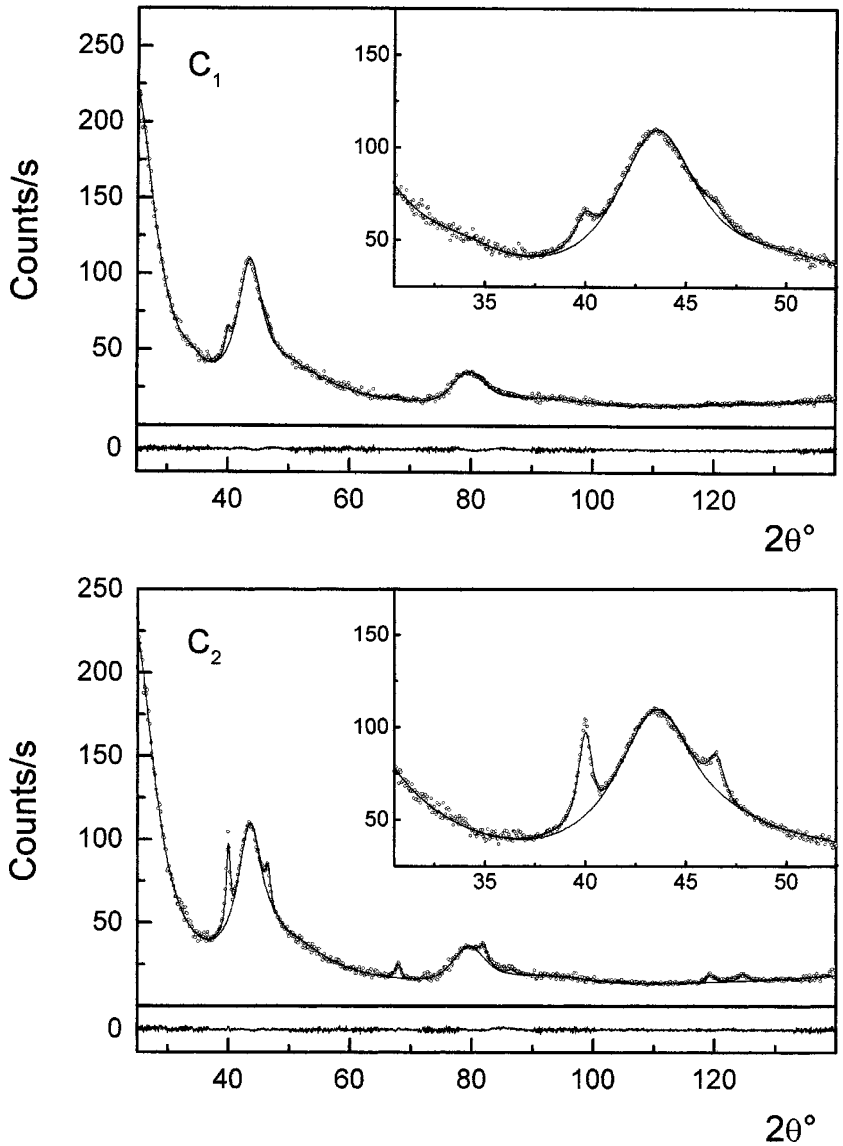

Figure 1. The XRD patterns of samples C_1 and C_2, fitted using our Rietveld procedure. In the insets the global diffuse scattering is evidenced, which represents the sum of Compton scattering, thermal diffuse scattering from the Pd phase, and smoothed experimental carbon scattering, suitably scaled. The weighted residuals, defined as $\Delta Y_i(\text{weighted}) = (Y_{\text{o}i} - Y_{\text{c}i})/Y_{oi}^{1/2}$, are reported at the bottom. The goodness of fit S is 1.1 for the Rietveld analysis of sample C_1 and 1.6 for that of sample C_2, where $S^2 = \{\sum_i [\Delta Y_i(\text{weighted})]^2\}/(N-P)$. The refined Pd unit cell edge, a, is 3.895(2) Å for sample C_1 and 3.896(1) Å for sample C_2 (see Young [19] for the symbol definitions). For reasons of graphics, the air-corrected experimental intensities are indicated by circles, spaced at 0.15° in 2θ.

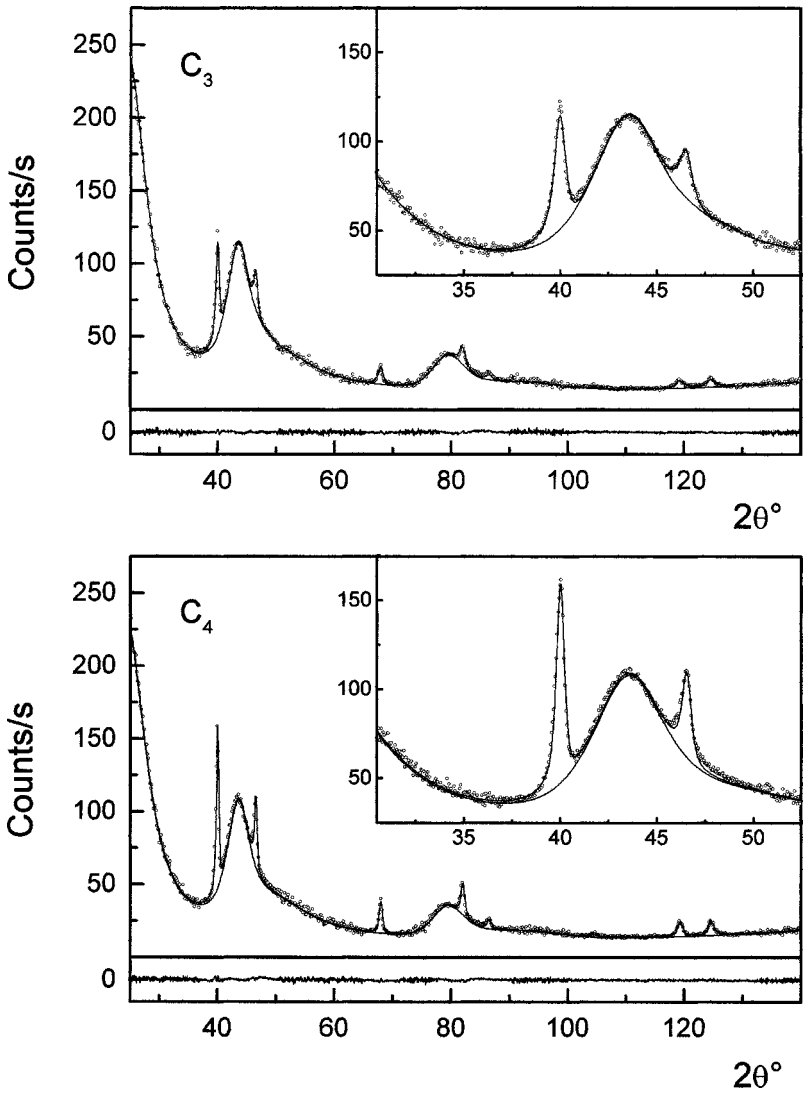

Figure 2. As in figure 1, but for C_3 and C_4 samples. For catalyst C_3 S and a are 1.5 and 3.897(1) Å, respectively, while for catalyst C_4, S and a are 1.7 and 3.8947(2) Å, respectively.

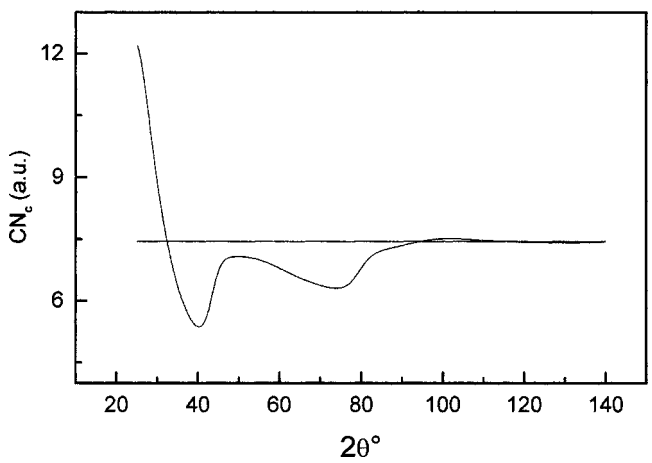

Figure 3. Plot of $CN_C(2\theta)$ (see equation (3)) relative to the active carbon used as a support for the investigated catalysts. The straight line represents the mean value of the curve evaluated in the region $2\theta > 100°$; this value is proportional to the number of composition units, assuming that one C atom is the composition unit of carbon.

which gives rise to the "visible" XRD peaks, determined by our approach: equation (5) was used to determine the CN_{Pd} quantity and equation (2) was used to determine the CN_C quantity. It is interesting to note, in the second column of table 1, that, for sample C_4, thermally treated at 873 K, the Pd content (0.50 wt%) is very close to the value obtained by the atomic absorption technique (0.51(2) wt%). This is proof that in this sample the sintering process made the Pd particles grow, so that almost all of them were responsible for the observed XRD peaks (practically no crystallite gives scattering outside the visible reflections). Therefore, this sample could be considered a correct reference sample for the single-peak method (see below). In contrast, in the "as received" catalyst, only 24% of Pd atoms (see column 3, table 1, where the "visible" Pd fraction, x, is reported) scatter inside the measurable XRD peaks. Evidently, the remaining fraction of atoms form nanoclusters which are so small that their scattering is diffused into the background. It is possible to see in the XRD pattern of

Table 1
Results obtained for the palladium fraction responsible for the "visible" XRD peaks, and for the relevant average crystallite sizes. The estimated percentage errors are 5% for W_{Pd} and 15% for $\langle D\rangle_{(111)}$ and $\langle D\rangle_{(100)}$.

Sample	Rietveld analysis		Single-peak analysis		
	Apparent Pd content	Pd fraction[a]	Crystallite size (Å)		Pd fraction[b]
	W_{Pd} (wt%)	x	$\langle D\rangle_{(111)}$	$\langle D\rangle_{(100)}$	x'
C_1 (as received)	0.12	0.24	68	n.d.	0.25
C_2 (673 K)	0.28	0.55	99	n.d.	0.64
C_3 (773 K)	0.34	0.67	123	108	0.68
C_4 (873 K)	0.50	0.98	143	143	1.00

[a] These values were obtained with reference to the real amount of 0.51 ± 0.02 wt% of palladium measured on the "as received" catalyst, using atomic absorption technique.
[b] These values were obtained with reference to sample C_4 (for which $x' \equiv 1$).

C_1 (figure 1) that, centred at about 34° in 2θ, there is a weak and diffuse halo which is due to PdO extremely fine particles, but this circumstance does not change the conclusions reported above. The C_2 and C_3 samples show an intermediate behaviour with respect to C_1 and C_4.

The right-hand side of table 1 shows the results obtained by means of the single-peak method. Using a published procedure [18] developed at our laboratory, we fitted the Pd(111) peak-profile in the angular 35°–50° range with a pseudo-Voigt function (intermediate between a Gaussian and a Lorentzian profile function) and the background with a second-order polynomial (see figure 3). By using the analytical Fourier transform of the profile, suitably desmeared from the instrumental broadening, the volume-weighted average crystallite size $\langle D\rangle_{(111)}$, measured perpendicularly to the (111) lattice planes, could be determined. For the two samples C_3 and C_4, the $\langle D\rangle_{(100)}$ average crystallite size, perpendicular to the (100) lattice planes, could also be de-

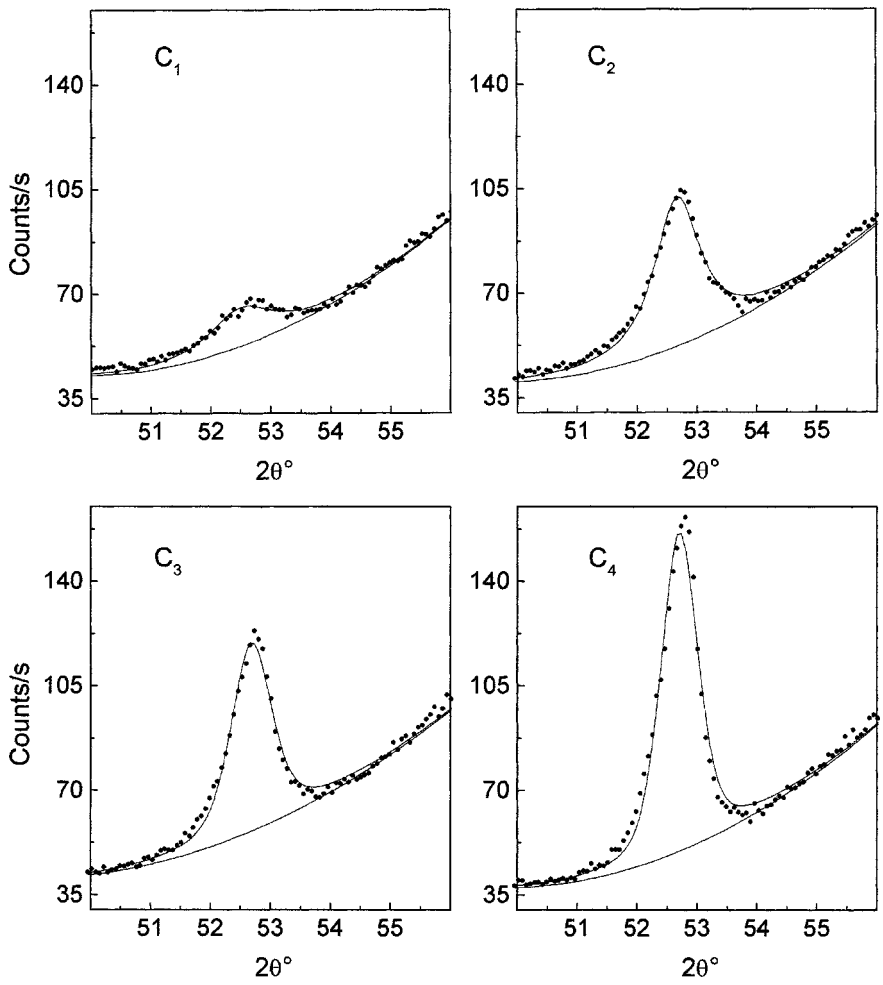

Figure 4. The fitted (111) palladium peak profiles of the four investigated samples C_1–C_4. Starting from the fitting data, the average volumetric crystallite sizes $\langle D\rangle_{(111)}$, reported in table 1, could be obtained.

termined because, in these two catalysts, the (200) XRD peaks were intense enough to be suitably fitted, and, therefore, studied in terms of line broadening. The line broadening was entirely ascribed to crystallite size broadening effects. In fact, an accurate analysis of lattice disorder, which is another possible cause of line broadening, cannot be performed on this kind of composite samples, where the metal amount is so low and the peaks so weak.

The crystallite values are reported in the fourth and fifth columns, respectively, of table 1. It is possible to note that the crystallite sizes systematically increase as the sintering temperature increases. Finally, the sixth column of table 1 gives the fraction of "visible" palladium, x', obtained from the ratio between the (111) peak area of the investigated sample and the corresponding area of sample C_4, considered as the reference sample for the series of catalysts; as a result, the x' values are very close to the x values, except for sample C_2. Therefore, this behaviour shows that, when crystal preferred orientations are not present, as verified here by the Rietveld refinements themselves, the relatively simple single-peak analysis (which is interesting for fast industrial applications) can give acceptable results, provided that the XRD experimental conditions remain constant. A nearly identical amount of powder should be put into the holder, for each sample, and the primary beam should be periodically checked using a standard reference sample, in order to take into account possible variations. Figure 4 shows the fitted profiles of the Pd(111) peaks of the four catalysts C_1, C_2, C_3 and C_4, reported in table 1.

5. Conclusions

For a quantitative determination of very fine metal particles or nanoclusters in metal supported catalysts, the X-ray Rietveld refinement, which is a complex, delicate and time-expensive technique, presents the following advantages with respect to simpler (relative) XRD methods, as the single-peak area measurement analysis:

(1) It is an absolute method that needs no reference sample nor constant experimental conditions.

(2) It can work well also in presence of crystal preferred orientations, which can be corrected by the method itself.

(3) It is much more precise since it is based on a full-pattern structural fitting technique.

The Pd fractions due to nanoparticles of 20–25 Å in size, as determined by the two above discussed methods, are close each other for all samples investigated, apart from one for which the disagreement is near 20%.

Acknowledgement

We are grateful to Ing. M. Cerboni of Chimet Co. (Arezzo, Italy), who supplied us with the "as received" catalyst and with the relevant active carbon used as support.

References

[1] P. Gallezot, in: *Catalysis, Science and Technology*, Vol. 5, eds. J.A. Anderson and M. Boudart (Springer, Berlin, 1984) ch. 4.
[2] R.J. Matyi, L.H. Schwartz and J.B. Butt, Catal. Rev. Sci. Eng. 29 (1987) 41.
[3] N. Pernicone, M. Cerboni, G. Prelazzi, G. Fagherazzi and F. Pinna, Catal. Today 44 (1998) 129.
[4] P. Riello, P. Canton and G. Fagherazzi, J. Appl. Crystallogr. 31 (1998) 78.
[5] P. Riello, G. Fagherazzi, D. Clemente and P. Canton, J. Appl. Crystallogr. 28 (1995) 115.
[6] R.J. Hill and C.J. Howard, J. Appl. Crystallogr. 20 (1987) 467.
[7] P. Riello, P. Canton and A. Benedetti, Langmuir 14 (1998) 6617.
[8] P. Riello, P. Canton, A. Benedetti and G. Fagherazzi, in: *Advances in X-Ray Analysis*, Vol. 42 (ICDD, Newton Square, PA, 1999), in press.
[9] V.H. Smith, Jr., A.J. Thakkar and D.C. Chapman, Acta Cryst. A 31 (1975) 391.
[10] W. Ruland, J. Appl. Phys. 15 (1964) 1301.
[11] P. Riello, P. Canton and G. Fagherazzi, Powder Diffr. 12 (1997) 160.
[12] G.W. Brindley, Philos. Mag. 36 (1945) 347.
[13] J.C. Taylor and C.E. Matulis, J. Appl. Crystallogr. 24 (1991) 14.
[14] S. Ottani, P. Riello and S. Polizzi, Powder Diffr. 8 (1993) 149.
[15] P. Riello, P. Canton and G. Fagherazzi, Powder Diffr. 10 (1995) 204.
[16] W. Ruland, Acta Cryst. 14 (1961) 1180.
[17] A. Sakthivel and R.A. Young, in: *User's Guide to Programs DBWS-9006PC* (Georgia Institute of Technology, Atlanta, GA, 1990).
[18] S. Enzo, G. Fagherazzi, A. Benedetti and S. Polizzi, J. Appl. Crystallogr. 21 (1988) 536.
[19] R.A. Young, in: *The Rietveld Method*, ed. R.A. Young (IUCR–Oxford Univ. Press, Oxford, 1993) ch. 1.